Lasers in Manufacturing Conference 2019

Laser blank-rim melting for robust laser welding of hidden T-joints with OCT-based position control

Mittelstädt C.[a*], Seefeld T[a], Vollertsen F.[b]

[a]*BIAS – Bremer Institut für angewandte Strahltechnik GmbH, Klagenfurter Straße 5, 28359 Bremen, Germany*
[b]*BIAS – Bremer Institut für angewandte Strahltechnik GmbH and University of Bremen, Klagenfurter Straße 5, 28359 Bremen, Germany*

Abstract

Laser-based blank-rim melting can be used to create reinforcements and increase the sheet thickness locally. This can be utilized to improve the robustness of laser welding of hidden T-joints, a more challenging joining task in terms of joint preparation. In this work laser welding of hidden T-joints using an OCT-based closed-loop position control is presented. Thereby, a lateral offset of 4.5 mm could be compensated and defect-free welding of hidden T-joints could be attained. Furthermore, it is demonstrated that using reinforced web-sheet edges increased the robustness of the closed-loop control significantly.

Keywords: welding; keyhole; sensing; process control, OCT

1. Introduction

The laser beam is one if not the most versatile tool in today's production, which is why it can be found in any manufacturing category. Whether it is original forming, shaping, cutting, joining, coating or changing material properties, laser material processing became economical for a lot of applications. That universal applicability is because of the laser beam's typical precise energy input and a continuously improving price-to-performance-ratio of available beam sources.

Aside from the mere heat treatment, laser melting applications can be distinguished between heat-conduction processes and deep-penetration processes (Poprawe, 2005). The latter regime is characterized by the formation of the so-called keyhole, a metal vapor capillary, which occurs when the energy density of

* Corresponding author. Tel.: +49-421-218-58030; fax: +49-421-218-58063.
E-mail address: mittelstaedt@bias.de

the laser beam exceeds an i. a. material-depending threshold-value (Zou *et al.*, 2015). Deep-penetration processes usually have an increased efficiency compared to heat-conduction processes due to an increased absorption of the laser beam energy inside of the keyhole (Wang *et al.*, 2017). However, it depends on the particular application which process variant is best suited for use.

One application that this contribution addresses is laser blank-rim melting to create reinforced blank-rims. Laser blank-rim melting enables to overcome the limits of conventional mechanical upsetting for some workpiece geometries, as demonstrated for rods by Brüning & Vollertsen, 2015 and blanks by Woizeschke *et al.*, 2015 with thicknesses between some ten microns and one millimeter. For workpieces with those dimensions, size effects can be exploited to attain conventionally unattainable upsetting ratios, see Vollertsen *et al.*, 2009. For laser-based upsetting processes, both heat-conduction and deep-penetration laser melting can be used, whereat more consistent shaping could be attained in the heat-conduction regime (Brüning, 2016). However, the use for reinforced blank-rims is diverse, including e. g. sheet-bulk metal forming (Merklein & Hagenah, 2016) and potentially hemming (Woizeschke *et al.*, 2018). In this contribution another application for blank-rim melting is pointed out, which is joint preparation for deep-penetration laser welding of hidden T-joints.

Laser welding of hidden T-joints can hardly be found in today's production due to high requirements in terms of clamping and process guidance to assure defect-free joining. Obviously, this is because the web-sheet and therefore the location of the joint is not visible from the face-sheet side. It could be demonstrated that i. a. a reinforced web-sheet edge allows to tolerate a slight misalignment between the travel path of the laser beam and the web-sheet (Mittelstädt *et al.*, 2018). However, a solution to compensate possible misalignment and assure defect-free welding of hidden T-joints is desirable. Lately, the introduction of optical coherence tomography (OCT) in laser material processing created a lot of opportunity for in-process measurement and closed-loop control (Kogel-Hollacher *et al.*, 2016). In fact, OCT-systems are already in use for seam tracking and position control for remote applications (Deyneka-Dupriez & Denkl, 2017). Furthermore, OCT is used for in-process measurement and closed-loop control of the weld depth in deep penetration laser welding applications (Bautze *et al.*, 2015). For the latter application, the OCT-data must be processed to extract the weld depth from the measuring data because the OCT-measurement not only contains data points from the bottom of the keyhole (Dorsch *et al.*, 2016).

This contribution presents an application for an in-process closed-loop control of a laser process using OCT. Thereby, the technology is adapted to distinguish between partial-penetration welding and full-penetration welding in laser joining of hidden T-joints. Based on that an event-based position control of the laser beam towards the web-sheet is realized. In this regard, another application for laser blank-rim melting which is preparing of the web-sheet for hidden T-joint-welding is pointed out.

2. Experimental

2.1. Material and method

In the presented investigations aluminum alloy EN AW-5083 sheet material was used. The utilized specimen were 150 mm in length, 50 mm in width and the sheet thickness was 1.5 mm. For laser welding of hidden T-joints an angular misalignment between the travel path of the laser beam and the web-sheet was adjusted (±4.5 mm at 150 mm sample length), **Fig. 1**. By this means, different regimes from full-penetration welding (welding next to the web-sheet) to partial-penetration welding (welding on the web-sheet) emerged depending on the position. This was analyzed using optical coherence tomography (OCT) for varying laser powers.

Furthermore, for the welding experiments the geometry of the utilized web-sheets was varied. In these investigations 3 mm and 5 mm wide trapezoidal-shaped reinforcements of the web-sheets were used, see **Fig. 1**. Each combination of laser power and web-sheet geometry was executed three times.

For these investigations, the reinforcements were created by milling down 3 mm and 5 mm thick base material to a waist-size 1.5 mm.

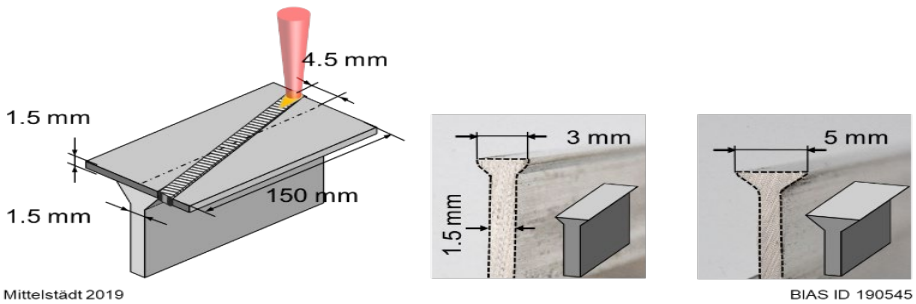

Fig. 1. left) schematic illustration of the sample and joint geometry, the adjusted angular misalignment; right)- utilized trapezoidal reinforcement geometries (3 mm and 5 mm).

2.2. Laboratory set-up

The beam source for the welding experiments was a TruDisk 12002 (optical fiber diameter 200 µm, 1030 nm wavelength) as well. Furthermore, an OCT-system In-Process Depth Meter (IDM; wavelength 1550 nm ±25 nm) from Precitec was used for weld depth measurement. The processing beam and the probe beam were aligned coaxially using a Precitec focusing optic YW52 with a tailor-made 45° beam splitter module, transmitting the probe beam radiation and reflecting the processing beam radiation (cf. **Fig. 2a**). The utilized IDM had a sampling rate of 70 kHz and a measuring range of 10 mm.

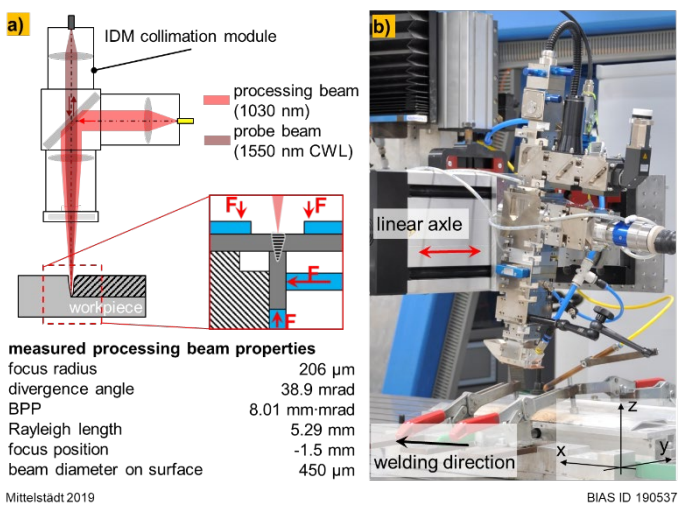

Fig. 2. a) Schematic illustration of the optical beam paths; b) Picture of the set-up for welding hidden T-joints.

The focusing optic had a magnification ratio of 2:1, adding up from a collimation focal length of 150 mm and a focusing focal length of 300 mm. The resulting processing beam properties were determined using a PRIMES high-power microspot monitor and are given in **Fig. 2a**. The processing beam focus position was set to -1.5 mm in relation to the surface of the specimen, resulting in a beam diameter of 450 µm on the surface

of the work piece. The utilized clamping device was adapted for welding hidden T-joints. Clamping levers were used to fix both the web-sheet and the face-sheet in flat position. Additionally, a spring seat was equipped to the clamping device to push the web-sheet against the face-sheet and thereby attain zero-gap conditions.

A picture of the welding set-up is given in **Fig. 2b**. Notice that the processing head was tilted about 5° in relation to the perpendicular axis in trailing configuration related to the process-feed in positive x-direction. Another important feature of the welding set-up was an additional linear axle to which the welding head was attached to. This axle was not used to realize the welding process feed but as part of a closed-loop position control which included the IDM as measuring device. Furthermore, for the welding experiments shielding gas argon was supplied with a flow rate of 10 l/min.

3. Results and discussion

3.1. Welding of hidden T-joints with angular misalignment

In **Fig. 3** the resulting raw data of an OCT measurement along with curves of processed measurands from this raw data is given for welding of hidden T-joints with angular misalignment between the travel path of the laser beam and the web-sheet (±4.5 mm at 150 mm sample length). Note that the utilized web-sheet had a reinforced edge (3 mm) which increased the contact area between the sheets. Therefore, the welding experiment featured geometrically distinguishable segments (cf. **Fig. 3a**). Full-penetration welding (area I – laser beam next to the web-sheet), transition-areas (area II – laser beam on the reinforcement) and partial-penetration welding (area III – laser beam on the web-sheet). Thereby, it could already be demonstrated that those transition areas facilitate to compensate slight misalignment increasing the process tolerance for welding of hidden T-joints (Mittelstädt *et al.*, 2018). In the following section it is elaborated, how to distinguish these segments by means of OCT.

Evaluating the OCT-data

Generally, an in-process weld depth measurement using OCT can feature a lot of measuring points from the process zone. The probe beam could be backscattered from both the keyhole and the sheet surface. The reason for that was discussed in previous publications, e. g. from Dorsch *et al.*, 2016. Therefore, signal processing is required to extract the desired information from the raw data, cf. Kogel-Hollacher *et al.*, 2016.

In **Fig. 3a** the position of the keyhole bottom (red curve) and the position of the work piece surface (magenta curve) were processed from the raw data (green data points) with the difference of both being considered as the measured weld depth. Thereby, the red curve was a 95 % percentile-fit (percentile rank number 95, considering a range of 750 raw data points) and the magenta curve was a histogram-fit which allowed to determine the position of the sheet surface to be at around 2 mm in the measuring range. Notice, that for a precise measurement of the actual weld depth a metallographic calibration is required, as previously shown by the authors (Mittelstädt *et al.*, 2019). However, for these investigations an accurate absolute value for the measured weld depth is less important than relative alterations of the measuring values.

Considering the percentile fit curve, it is worthy noting that it was constantly below 3.5 mm in the measuring range. Related to the determined surface position (2 mm ±0.1 mm), this resulted in a measured weld depth larger than the sheet thickness of 1.5 mm. Apart from background noise, the occurrence of raw data values larger than 3.5 mm in the full-penetration area could either be attributed to multiple reflected measuring radiation from the keyhole, or sagging of the melt, which can occur in this regime (Nothdurft *et al.*, 2018). However, by considering the course of the percentile curve it is not possible to distinguish reliably between full-penetration and partial-penetration welding with values around 4 mm distance existing along the entire measurement. However, to do so another measurand computed from the raw data has to be found.

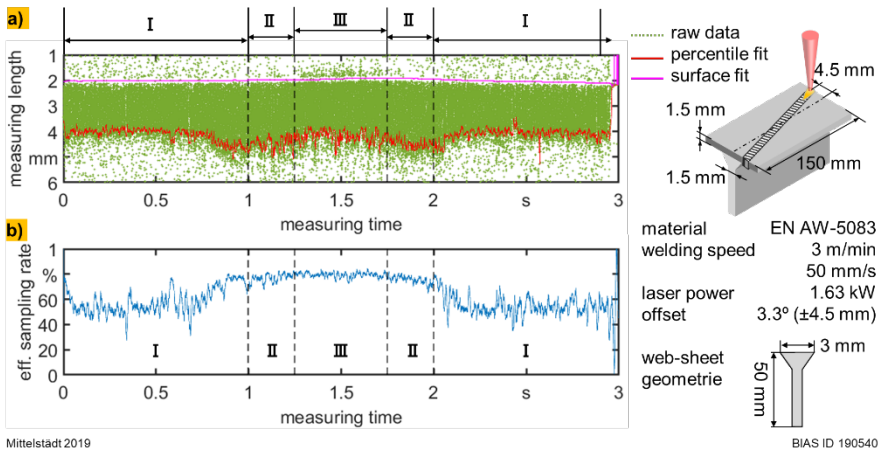

Fig. 3. OCT-measurement for welding a hidden T-joint with dedicated angular misalignment between the web-sheet and the travel path of the laser beam. a) raw data superposed with 95 % percentile curve (red line) which indicates the keyhole/weld depth and a histogram fit curve (magenta line) which indicates the sheet surface; b) resulting effective sampling rate.

Effective sampling rate

The effective sampling rate (depicted in **Fig. 3b**) turned out to be suitable to distinguish between partial-penetration and full-penetration welding. This measurand is computed by considering the number of attained raw data points and the sampling rate of the OCT-sensor (70 kHz) for the same interval. According to the computation of the percentile curve, a range of 750 data points (corresponding to a time of ~0.01 s) was considered to calculate the effective sampling rate. **Fig. 3b** illustrates that the effective sampling rate is more constant and on a higher level (~80 % ±3 %) in the range of the web-sheet than it is in the range of full-penetration welding (~52 % ±12 %). The possibility to identify the position of the laser beam relative to the web-sheet is discussed in the following section for a varying laser power.

Variation of the laser power

To begin with, the OCT-measurement was used to identify four laser power adjustments which resulted in four different desired weld depths. the correlation between the utilized laser power and the resulting weld depth for the given application is shown in **Fig. 4**. Here, welding took place without misalignment. Four laser powers (1.38 kW, 1.68 kW, 1.88 kW 2.13 kW) were identified which led to purposefully staggered mean weld depths of 1.8 mm, 2.25 mm, 3 mm and 3.5 mm. The selection was made with respect to the sheet thickness of 1.5 mm. Those laser powers were used for welding with angular misalignment.

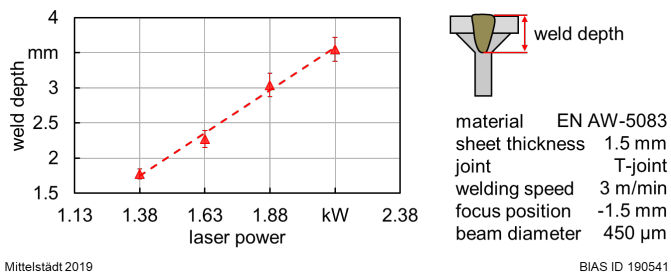

Fig. 4. Measured weld depth as a function of the laser power for welding of hidden T-joints without misalignment.

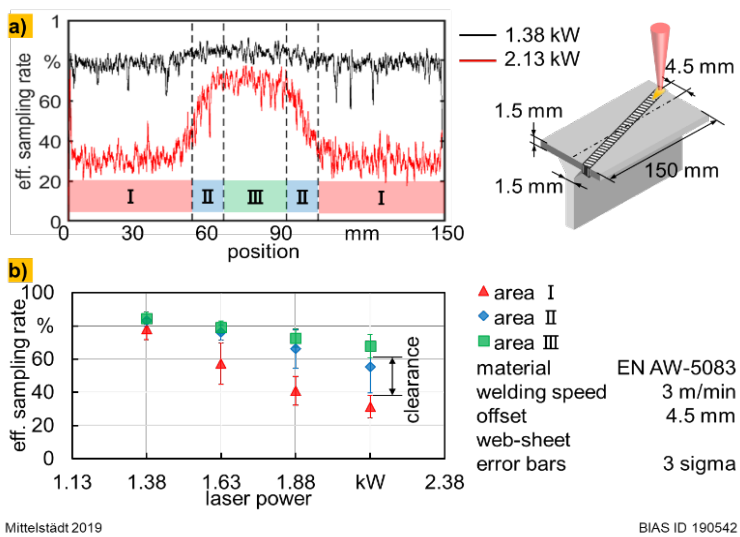

Fig. 5. a) Comparison of the course of the effective sampling rate for welding with angular misalignment using different laser powers. b) Mean values of the effective sampling rate by area for varying laser power.

Distinguishing full-penetration and partial-penetration welding

Fig. 5 compares OCT-measurements for welding with angular misalignment for varying laser power. In **Fig. 5a** the course of the effective sampling rate is given representatively for both ends of the investigated laser power span, i. e. 1.38 kW and 2.13 kW. The comparison shows that the discrimination between

full-penetration and partial-penetration welding (area I & area III) is easier for the higher laser power. Furthermore, for the higher laser power a transition area between the two regimes is apparent (area II – laser beam in range of the reinforcement).

In **Fig. 5b** the analysis of the computed effective sampling rates with respect to the position of the laser beam towards the web-sheet is summarized for the investigated laser powers. It is evident that the effective sampling rate is depending on both the position and the laser power. Overall, the effective sampling rate decreased with increasing laser power for each of the discriminated areas. Considering the partial-penetration mode (area III), the decreasing effective sampling rate with increasing laser power can be attributed to an increasing keyhole depth. Dorsch *et al.*, 2016 discussed the same trend in their investigations. The trend can be explained by an increasing absorption of the measuring radiation – and therefore less backscattered radiation which is mandatory for measuring – as discussed by Wang *et al.*, 2017. In fact, this was discussed for the processing laser radiation, however the same trend should also apply for the probe beam radiation. Moreover, the decreasing effective sampling rate showed also in the other areas of the welds. In case of full-penetration welding, this is most likely due to a widening keyhole-bottom opening for increasing laser power. This correlation was illustrated e. g. by Zhang *et al.*, 2018.

To use the effective sampling rate for a robust closed-loop position control, a clearance between the values for full-penetration welding (area I) and partial penetration welding (area III) is desired. However, the variance of the effective sampling rate must be taken into account to rule out unwanted trigger-events in case of being in the right position and short-term threshold exceeding in case of being in the wrong position. Therefore, the clearance was defined as the gap between the scattering (considered 3 times the standard deviation) of the measured effective sampling rates in area I and area III, see **Fig. 5b**.

Reliable distinguishing for robust position-control

The clearance has been investigated for varying laser power and different web-sheet geometries, considering different sized reinforcements and conventional web-sheets. The results are given in **Fig. 6**. For the lowest investigated laser power of 1.38 kW, the clearance was below zero for all considered web-sheet geometries. This means that the error bars of the respective effective sampling rates were lapping, allowing no proper threshold value for a robust position control. Given the course of the effective sampling rate illustrated in **Fig. 5a,** for 1.38 kW this was expectable. However, for increasing laser power the clearance increased above zero which illustrates the possibility for a robust closed-loop control using the effective sampling rate as reference value. Thereby, the largest clearances were determined for 2.13 kW. However, at this laser power level the weld depth was twice the thickness of the sheets which could be considered inappropriate. For both intermediate laser powers (1.63 kW and 1.88 kW) the 3 mm reinforcement of the web-sheet was best suited to establish a clearance. Compared to the clearances determined for the web-sheet without reinforcement, this could be explained by a smoother transition of the effective sampling rate from full-penetration welding to partial-penetration welding, vice versa. Furthermore, the determined effective sampling rates were more constant in the range of the web-sheet (area III) for welding with a reinforcement than without. Moreover, **Fig. 5b** illustrates for the intermediate laser powers that the error bars of web-sheet area (area III) and those of the reinforcement area (area II) are lapping. Therefore, given a sensitive-parametrized threshold value, welding in the reinforcement area could already trigger the closed-loop control which would facilitate to compensate even slight misalignments.

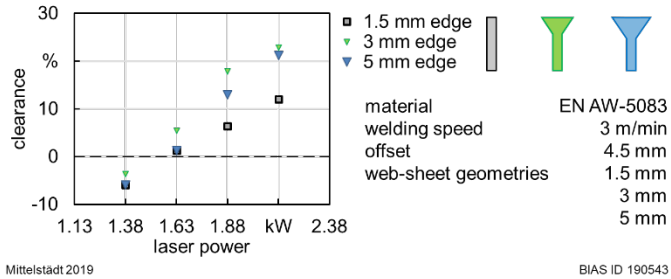

Fig. 6. Clearance between measured effective sampling rates including scattering for full-penetration welding (area I) and partial-penetration welding (area III).

All in all, **Fig. 6** illustrates that a reinforcement of the web-sheet is beneficial for welding hidden T-joints in terms of finding an appropriate threshold for the reference value of a closed-loop position control. Especially for lower laser powers and appropriate weld depths, the use of a reinforcement is lucrative. To create those reinforcements laser blank-rim melting is an interesting solution, as Woizeschke *et al.*, 2018 pointed out that the process is suitability to attain preforms with diameters of easily twice the thickness of the used blank. However, it is expedient to mold the cylindrical preforms in a further step to attain reinforcements with a flat flange facing to increase the contact area between the web-sheet and the face-sheet. This could be achieved either by milling the top-part of the preform or shaping it e. g. by means of a subsequent (hot-)rolling process.

Yet, a robust position control can be achieved above 1.63 kW even without a reinforcement given an accurately set threshold value. Using the effective sampling rate as reference value for a closed-loop control is demonstrated in the following section.

OCT-based closed-loop position control

Fig. 7 illustrates the result and the operating principle of the closed-loop position control. For the given example a lateral offset of 4.5 mm at 120 mm seam length was adjusted. Furthermore, a laser power of 1.63 kW was used and the geometry of the web-sheet was without reinforcement.

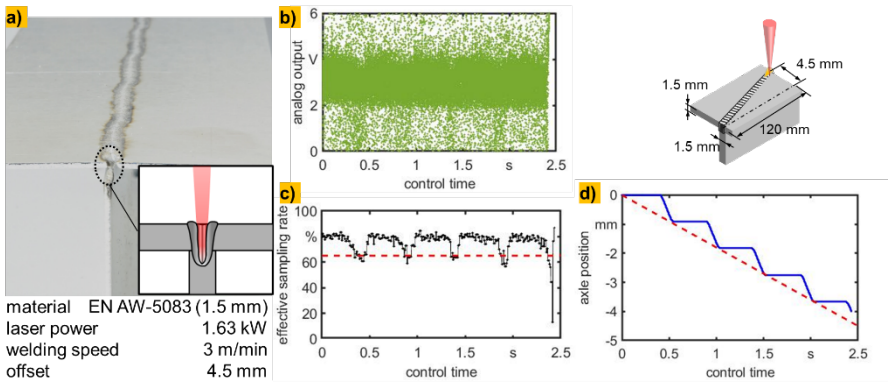

Fig. 7. a) Hidden T-joints specimen welded with OCT-based position control; b) Raw data analog output signal from the OCT-system; c) Computed effective sampling rate from the raw data; d) position adjustment by the additional linear axle.

Fig. 7a shows a welded sample featuring a wavy top-bead of the seam with the end of it being atop of the web-sheet. Hence, the adjusted lateral misalignment was compensated. The responsible closed-loop position control considered the analog output signal from the OCT weld-depth measurement (**Fig. 7b**), computed the effective sampling rate from it (**Fig. 7c**) and in case of falling below the given threshold value of 65 % the additional linear axle (see **Fig. 2b**) was used to adjust the position (**Fig. 7d**). For the analog output signal 1 V was equivalent to 1 mm in the weld depth measurement. The resulting effective sampling rate was around 80 % for the laser beam in the range of the web-sheet. Falling below 65 % triggered the position adjustment which moved the laser beam back towards the web-sheet. In the depicted case, the position control was iterative using 0.75 mm steps (half the thickness of the web-sheet) with a positioning velocity of ~6 mm/s which was enough to compensate the adjusted deposition velocity of ~1.88 mm/s (4.5 mm in 2.4 s).

Considering the direction of the position adjustment, the closed-loop position control uses one previously set direction for the first iteration. In case the position adjustment is not successful in the first iteration, the closed-loop control flips the direction of the position adjustment and uses a larger step width for the second iteration. Furthermore, the number of executed iterations is considered for the next trigger-event. Therefore, the closed-loop control is adaptable and generally suitable for future industrial use.

4. Summary

It could be demonstrated that OCT is feasible to distinguish between partial-penetration and full-penetration laser welding by considering the effective sampling rate of the measurement. Therefore, this metrology could be used successfully as a feedback element in a closed-loop position control of the laser beam in welding of hidden T-joints. Reinforcements of the web-sheet can be used to increase the contact zone between the web-sheet and the face-sheet which simplified distinguishing between partial-penetration and full-penetration laser welding by means of the effective sampling rate.

Acknowledgements

The IGF-Project no.: 19.626 N / DVS-No.: 06.111 of the “Forschungsvereinigung Schweißen und verwandte Verfahren e.V.” of the German Welding Society (DVS), Aachener Str. 172, 40223 Düsseldorf was funded by the Federal Ministry for Economic Affairs and Energy (BMWi) via the German Federation of Industrial Re-

search Associations (AiF) in accordance with the policy to support the Industrial Collective Research (IGF) on the orders of the German Bundestag. Furthermore, the authors gratefully acknowledge the collaboration with the members of the project affiliated committee regarding the support of knowledge, material and equipment over the course of the research.

The "BIAS ID" nos. are part of the figures and allow the retraceability of the results with respect to mandatory documentation required by the funding organization.

References

Bautze T., Moser R., Strebel M. & Kogel-Hollacher M. (2015) Use of inline coherent imaging for laser welding processes: Process control and beyond. In: *Lasers in Manufacturing Conference 2015* (ed. by T. Graf, C. Emmelmann, L. Overmeyer & F. Vollertsen).

Brüning H. (2016) *Prozesscharakteristiken des thermischen Stoffanhäufens in der Mikrofertigung.* BIAS Verlag.

Brüning H. & Vollertsen F. (2015) Energy efficiency in laser rod end melting. In: *Lasers in Manufacturing Conference 2015* (ed. by T. Graf, C. Emmelmann, L. Overmeyer & F. Vollertsen).

Deyneka-Dupriez N. & Denkl A. (2017) Advances of OCT Technology for Laser Beam Processing. *Laser Technik Journal,* **14,** 34–38. DOI: 10.1002/latj.201700021.

Dorsch F., Harrer T., Haug P. & Plasswich S. (2016) Process Control using Capillary Depth Measurement. In: *ICALEO 2016 Congress Proceedings: 35th International Congress on Laser Materials Processing, Laser Microprocessing and Nanomanufacturing*.

Kogel-Hollacher M., Schoenleber M., Bautze T., Strebel M. & Moser R. (2016) Measurement and Closed-Loop Control of the Penetration Depth in Laser Materials Processing. In: *Physics Procedia: Laser Assisted Net Shape Engineering 9* (ed. by M. Schmidt, F. Vollertsen & C.B. Arnold). Elsevier.

Merklein M. & Hagenah H. (2016) Introduction to sheet-bulk metal forming. *Production Engineering,* **10,** 1–3. DOI: 10.1007/s11740-016-0661-z.

Mittelstädt C., Mattulat T., Seefeld T. & Kogel-Hollacher M. (2019) Novel approach for weld depth determination using optical coherence tomography measurement in laser deep penetration welding of aluminum and steel. *Journal of Laser Applications,* **31,** 22007. DOI: 10.2351/1.5082263.

Mittelstädt C., Seefeld T., Woizeschke P. & Vollertsen F. (2018) Laser welding of hidden T-joints with lateral beam oscillation. *Procedia CIRP,* **74,** 456–460. DOI: 10.1016/j.procir.2018.08.151.

Nothdurft S., Springer A. & Kaierle S. (2018) Influencing the Weld Pool During Laser Welding. In: *Advances in Laser Materials Processing: Technology, Research and Applications* (ed. by J.R. Lawrence), pp. 235–256. Woodhead Publishing.

Poprawe R., editor (2005) *Lasertechnik für die Fertigung: Grundlagen, Perspektiven und Beispiele für den innovativen Ingenieur.* Springer, Berlin, Heidelberg.

Vollertsen F., d. Biermann, Hansen H.N., Jawahir I.S. & Kuzman K. (2009) Size effects in manufacturing of metallic components. *CIRP Annals,* **58,** 566–587. DOI: 10.1016/j.cirp.2009.09.002.

Wang H., Nakanishi M. & Kawahito Y. (2017) Effects of welding speed on absorption rate in partial and full penetration welding of stainless steel with high brightness and high power laser. *Journal of Materials Processing Technology,* **249,** 193–201. DOI: 10.1016/j.jmatprotec.2017.06.014.

Woizeschke P., Brüning H. & Vollertsen F. (2015) Lasergenerierte Blechkanten, **5,** 22–24.

Woizeschke P., Heinrich L. & Eichner P. (2018) Laser edge forming to increase the bending radius in hemming. *MATEC Web of Conferences,* **190,** 2002. DOI: 10.1051/matecconf/201819002002.

Zhang Y., Li F., Liang Z., Ying Y., Lin Q. & Wei H. (2018) Correlation analysis of penetration based on keyhole and plasma plume in laser welding. *Journal of Materials Processing Technology,* **256,** 1–12. DOI: 10.1016/j.jmatprotec.2018.01.032.

Zou J.L., He Y., Wu S.K., Huang T. & Xiao R.S. (2015) Experimental and theoretical characterization of deep penetration welding threshold induced by 1-μm laser. *Applied Surface Science,* **357,** 1522–1527. DOI: 10.1016/j.apsusc.2015.09.198.